STUDIA UBB CHEMIA, LXII, 3, 2017 (p. 165-176)
(RECOMMENDED CITATION)
DOI:10.24193/subbchem.2017.3.13

In memory of prof. dr. Simion Gocan

INFLUENCE OF THE COBALT NITRATE:ETHYLENE GLYCOL MOLAR RATIO ON THE FORMATION OF CARBOXYLATE PRECURSORS AND COBALT OXIDES

THOMAS DIPPONG[a], FIRUTA GOGA[b *], ALEXANDRA AVRAM[b]

ABSTRACT This paper focuses on the obtaining of carboxylate precursors through the redox reaction of cobalt nitrate and ethylene glycol, in different stoechiometric ratios, as well as the decomposition of precursors into cobalt oxides. The influence of the NO_3^-:$C_2H_6O_2$ stoichiometric ratio on the formation of the precursors is studied through thermal analysis, FTIR spectroscopy and acido-basic analysis (conductometric/potentiometric titrimetry). Phase analysis by XRD and FTIR of the powders obtained at the decomposition of the precursors at 400°C has evidenced the formation of CoO for a high NO_3^-:$C_2H_6O_2$ synthesis ratio and of Co_3O_4 for a low NO_3^-:$C_2H_6O_2$ ratio. The Scherrer equation and scanning electron microscopy (SEM) were used to determine the dimensions of the nanoparticles obtained.

Keywords: *carboxylate precursors, cobalt oxide, acido-basic titration*

INTRODUCTION

Nanomaterials have been the subject of intense research due to their many fascinating properties that are not attainable by bulk materials. Due to their exceptional attributes and reduced dimensions, they can be exploited in a large range of fields [1].

[a] *Technical University of Cluj-Napoca, Faculty of Sciences North University Center at Baia Mare, 76 Victoriei Street, 430122 Baia Mare, Romania.*
[b] *Babeş-Bolyai University, Faculty of Chemistry and Chemical Engineering, 11 Arany Janos Street, RO-400028, Cluj-Napoca, Romania.*
[*] *Corresponding author: firutagoga@yahoo.com*

Cobalt oxides are important materials with a wide array of applications, such as, catalysts [2, 3, 4, 5, 6], different kind of sensors [7, 2, 4, 5], lithium ion batteries [8,7, 5], optoelectronic devices [9,10], combustion of hydrocarbons at gas purification [11], supercapacitors [12,13], Fisher-Tropsh syntheses [14] and biomedical sciences [1,7,12]. Cobalt oxides obtained as nanoparticles present a particular interest due to their different properties compared to the bulk material. Obtaining methods for the cobalt oxid nanoparticles Co_xO_y are mentioned in scientific literature: the pyrolytic process [15], the combustion method [16, 17, 18, 4], the mechanico-chemical method [19], the hydrothermal method [4], pyrolytic spraying technique [20, 6], photochemical synthesis [21], sonochemical synthesis [13] etc.

In this paper we are following to obtain cobalt oxide nanoparticles through the decomposition of some carboxylate type complex combinations resulted in the redox reaction between $Co(NO_3)_2 \cdot 6H_2O$ and $C_2H_6O_2$. The influence of the NO_3^- **:** $C_2H_6O_2$ molar ratio on the formation of the oxidation products, precursors of cobalt oxides, and on the composition of the oxide system Co_xO_y obtained by thermal decomposition of the precursors has been studied. For the characterization of the precursors thermal analysis, FTIR spectrometry, XRD, SEM and acidic-basic titrations were employed.

RESULTS AND DISCUSSION

This paper studies the redox reaction between $Co(NO_3)_2$ and ethylene glycol, at different NO_3^- **:** $C_2H_6O_2$ molar ratios: 4**:**1 (sample D_1), 2:1 (sample D_2), 1.33**:**1 (sample D_3) and 1**:**1 (sample D_4).

The progress of the NO_3^- - $C_2H_6O_2$ redox reaction in all cases (D_1 – D_4) was followed with a thermal analysis. The cobalt nitrate – ethylene glycol solutions were submitted to a thin layer deposition on platinum trays and heated in air up to 500°C. Figure 1 presents the TG and DTA curves obtained for samples: D_1, D_2, D_3 and D_4. TG curves register two distinct mass loss steps, the first one, going up to 120 ^oC, is attributed to the decomposition of $Co(NO_3)_2$ and the volatilization of crystallization water. The second step, in between 200 and 260 ^oC, is attributed to the oxidative decomposition of the formed complex combination. This decomposition develops with a high speed in a short amount of time, generating a *in situ* reductive atmosphere that induces the reduction of Co(II) to metallic Co. Metalic Co further reoxidates to a weak crystallized oxide with increased reactivity [22].

The TG curve shows that the glyoxylate forming stoechiometric sample presents the lowest mass loss, whereas the glycolate forming stoechiometric sample presents the highest mass loss.

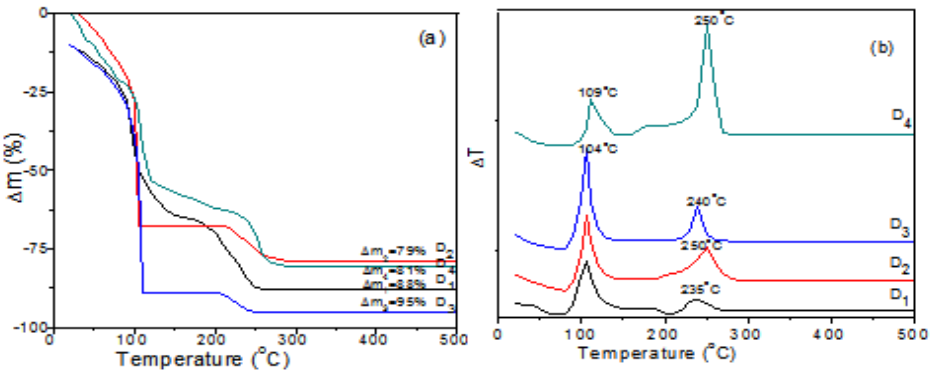

Figure 1. Thermogravimetric curves for $D_1 \div D_4$ (a) TG and (b) DTA

From the evolution of the DTA curves it can be observed that in all cases, regardless of the $Co(NO_3)_2 – C_2H_6O_2$ molar ratio, two exothermic efects are registered, corresponding to mass losses on the TG curve. The first such effect, with a maximum between 104-110°C corresponds to the NO_3^- - $C_2H_6O_2$ redox reaction, with the formation of compounds (Co (II) combinations with ethyleneoxide oxidation products). The second effect, with a maximum between 235-250°C, corresponds to the oxidative decomposition of the formed compounds. Following the thermal analysis data, it was established that the optimal synthesis temperature of these compounds is 130°C.

The purified products were analysed by FTIR spectrometry. Figure 2 presents the FTIR spectra for samples $D_1 \div D_4$, obtained at 140°C and 300°C. The FTIR spectrum for D_1 obtained at 140°C presents bands that are characteristic to $(NO_3)^-$ vibrations (1384 cm^{-1}), showing that for this sample, the carboxylate precursor was not completely formed. The FTIR study of the precursors has evidenced the presence, in all four cases, of the characteristic vibrations of carboxylate groups: ν_{as} (COO^-) at 1646-1588 cm^{-1} and ν_s (OCO) at 1316-1352 cm^{-1} [23]. The OH bonds in the carboxylate precursors are asociated with the 3380-3410 cm^{-1} and 881-790 cm^{-1} wavelenght numbers [23] respectively. The vibrations of the C-O bonds are also identified at 1063-1065 cm^{-1} [10]. For samples D_1 and D_2 bands corresponding the Co-O bond cand be observed at 490 cm^{-1} [10]. The FTIR spectra for samples D_3 and D_4, thermally treated at 300°C, do not show any bands characteristic to cobalt carboxylates. Samples D_1 and D_2 show traces of these bands at 1360 cm^{-1}, attributed to the thermal decomposition and the formation of the metalic oxide. All samples evidentiate intense bands at 663 cm^{-1} and 570 cm^{-1}, corresponding to the vibration of the Co-O bond.

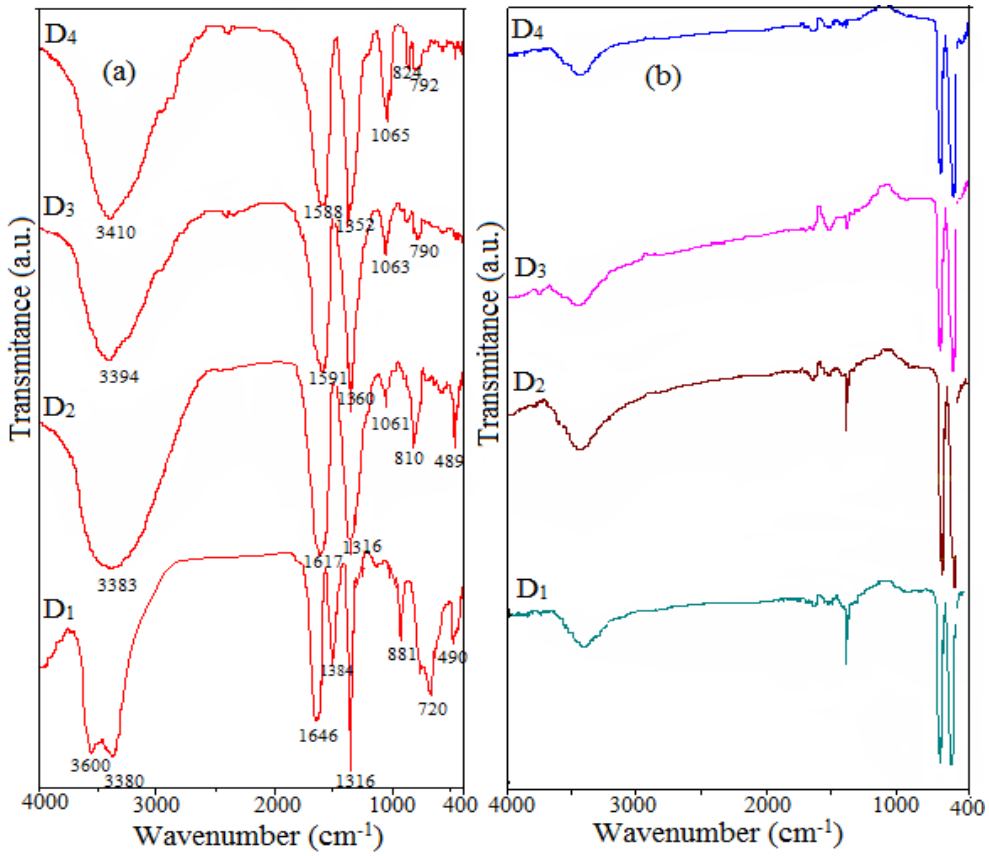

Figure 2. FTIR spectra of samples D1÷D4 at a)140°C and b) 300°C

Factoring in the reactants' ratio and the reaction conditions, the ethylene glycol oxidation can produce cobalt oxalate (CoC_2O_4), cobalt glyoxylate ($Co(CHOHCOO)_2$), or a mixture of the both (the acido-oxalate form is excluded). The cobalt (II) may occur in neutral form Co^{2+}, hydrolized ($CoOH^+$), as a hydroxide $Co(OH)_2$, or as a mixture.

For the study of the acido-basic properties, the 4 compounds, D_1-D_4, were treated with a 0,1M HCl solution. It was observed that they have different solubilities. Samples D_3 and D_4 solubilize completely, whereas samples D_1 and D_2 solubilize partially. The insoluble phase was filtered, washed, and submitted to a FTIR analysis. The FTIR spectra (Figure 3) of samples D_1 and D_2 evidentiates vibration bands typical to cobalt oxalate (1620 cm^{-1}, 1360 cm^{-1}, 1320 cm^{-1}, 820 cm^{-1}, 480 cm^{-}) [17].

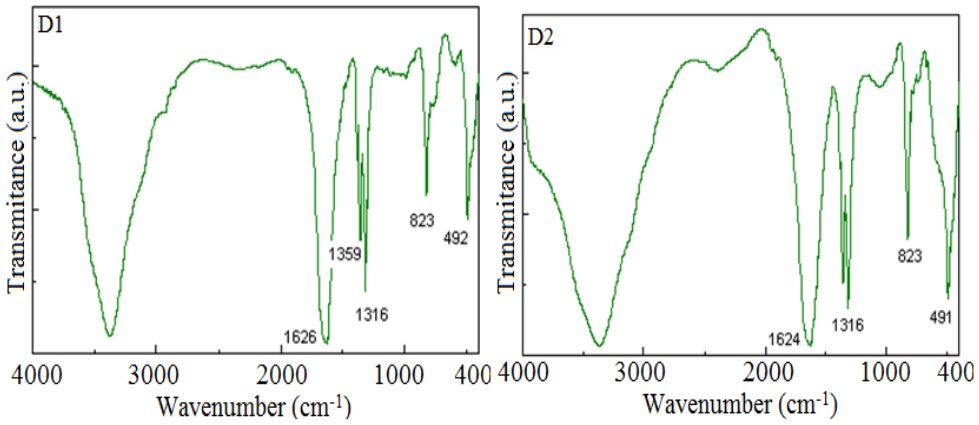

Figure 3. FTIR spectra of the HCl insoluble components of precursors D_1 and D_2

Furthering the supposition that samples D_1 and D_2 produce oxalates, the acido-basic properties of these compounds were focussed on. These can be determined by the ratio of HCl mols consumed while disolving and protonation of the precursors and the NaOH mols consumed for the $Co(OH)_2$ precipitation. The following reactions, establishing the H^+/HO^- ratios (acid quantity and consumed base) are hypotesized:

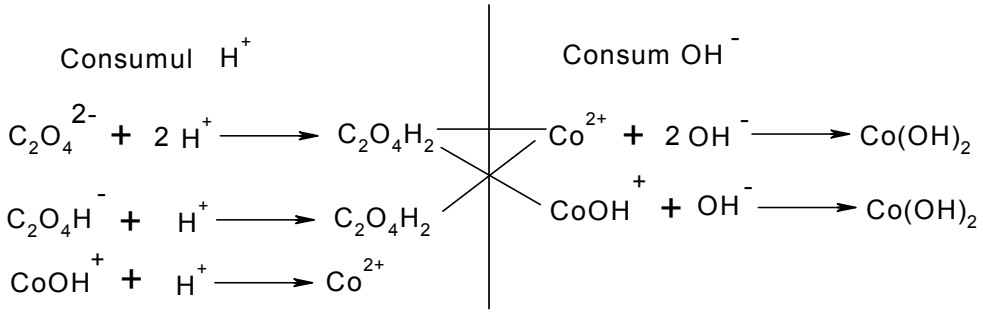

Scheme 1. The processes which may occur when the precursor was treated with HCl (left) and NaOH (right)

From the presented reactions one can calculate the theoretical ratio r = moles of HCl/moles of NaOH for the different possible species: CoC_2O_4 (r = 1/1), $[Co(OH)]_2C_2O_4$ (r = 2/1) or $Co(HC_2O_4)_2$ (r = 1/2).

Figure 4 presents the conductometric curves for D1-D4.

On the titration curves in Figure 4, two sets of data can be observed, the first corresponding to the ‚standard' titration, HCl with NaOH, formed by 2 lines with a single equivalence volume at ~ 10 cm^3. The second set corresponds to the (sample + HCl) NaOH titration, the

conductometric, curve being formed by 3 lines with 2 equivalence volumes. The lines were evidenced between the mean conductance points, corrected with the dilution volume (100 cm^3). Each graph contains a titration curve of the analized compound and a titration reference for the 2 reactants (acid/ base). There are 2 equivalence points for the sample, namely V_{e1}, V_{e2}, and one for the reference, V_{eR}.

On the pH metric curves (Figure 5), 2 sets of data are also observed. The first set corresponds to the HCl-NaOH reference, with a single saltation with the equivalence volume around 10 cm^3. The second set corresponds to the (sample + HCl) NaOH titration, presenting 2 pH saltations consistent with the 2 equivalence volumes.

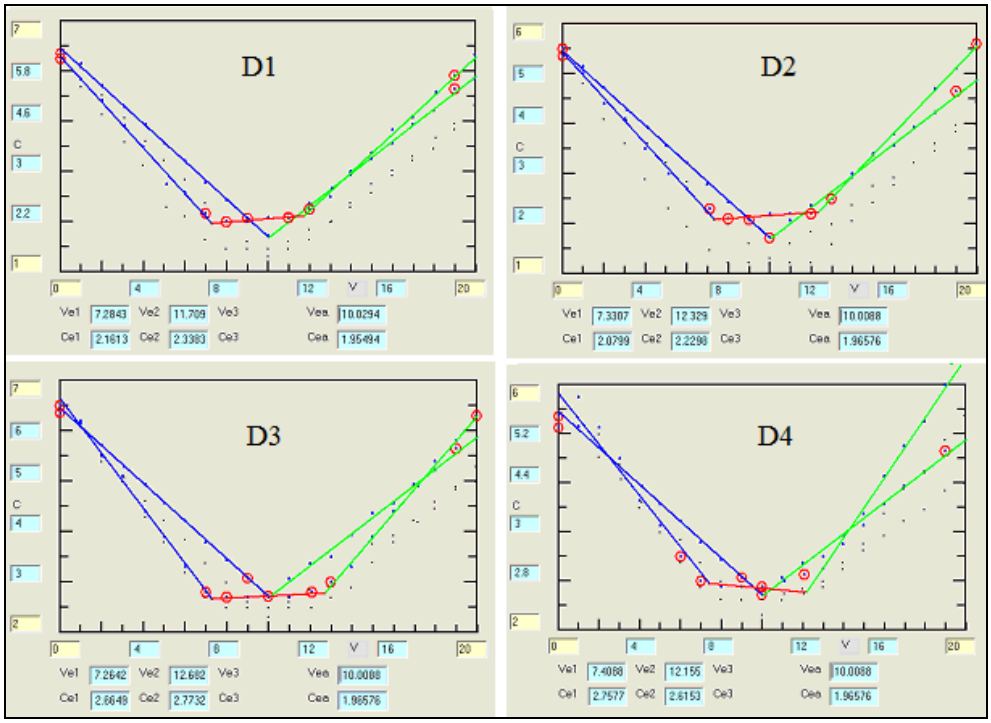

Figure 4. The conductometric titration curves for the Hcl titration with NaOH and the titration of samples D_1-D_4 with NaOH in HCl

The 3 sets of data from the conductometric titration were statistically processed. For calculating the acid/ base consumption, the R ± sR = (VeR ± sVeR) - (Ve1 ± sVe1)/ (Ve2 ± sVe2)-(VeR ± sVeR) formula is applied. Table 1 presents the acid/ base consumption ratios that resulted from the acido-basic titrations, for all 4 analysed samples.

The ratio of the acid consumption/ base consumption for sample D_1 differs from the rest of the samples. This corresponds to the fact that a mixture of basic oxalate and neutral oxalate is obtained. The formation of these 2 cobalt oxalates is explained by the existence of the metal ion $MeOH^+$ in equilibrium. At a certain pH level, hydrolysed metal ions appear in equilibrium, and if the solubility of the 2 oxalates are aproximately the same, both oxalates will precipitate.

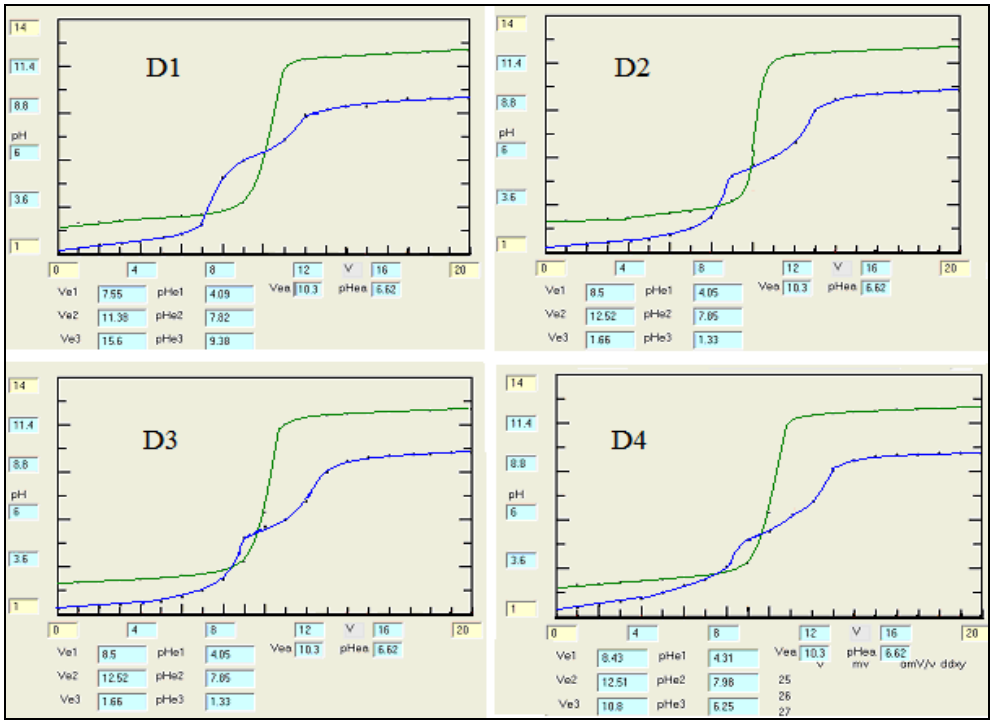

Figure 5. Potentiometric titration curves for the HCl – NaOH titration (green), and the NaOH titration of D_1-D_4 samples in HCl (blue)

Table 1. The acido-basic species formed during the conductometric and pH metric titrations

Sample	Conductometry ratio formed species	pH-metry ratio formed species
D1	1,8± 0.3 oxalate basic oxalate	1,6± 0.3 oxalate basic oxalate
D2	1,1± 0.3 oxalate	1,1± 0.3 oxalate
D3	1.0± 0.1 glyoxylate	1,0± 0.3glyoxylate
D4	1,2± 0.2 glyoxylate	1,0± 0.3 glyoxylate

The mixture of the 2 oxalates will lead to a ratio between 1-2. The basic oxalate forms through the the partial hydrolization of the metal ion resulted from the oxidation process, leading to more acid being consumed than base. In the case of sample D_2, considering that the acid/ base ratio is close to 1:1, only neutral oxalate is formed. At $Co(NO_3)_2/C_2O_2H_6$ ratios that differ from 4/3, mixtures of neutral oxalate salts and cobalt glyoxylate will result, in different ratios. At an excess of diol, only cobalt glyoxylate will result.

The acido-basic properties of the synthetised compounds correspond to the thermal analysis and FTIR spectra, confirming that carboxylate and hidro-carboxylate precursors are formed in the redox reaction, coordinating Co(II) ions in different acidic or basic compounds.

After the clarification of the precursor's nature, of the decomposition and thermal treatment conditions, the ways in which CoO and Co_3O_4 can be obtained as single phases are being followed.

D_1-D_2 precursors were thermally treated in air at 300°C for 2h, obtaining single oxide phases (CoO, Co_3O_4) or a mixture comprised of the two. Figure 6 presents the XRD spectra for samples D_2 and D_4, thermally treated at 300, 400 şi 700°C for 3h. Following the decomposition (20°C/min) and the thermal treatment of D_2 at 300 şi 400°C, CoO is obtained as a single, crystaline phase (JCPDS chart 75-0393 [24,25]). If the thermal treatment goes to 700°C, it is observed that CoO oxidises to Co_3O_4 (Figure 6a). For precursor D_4, following the same heating pattern, it is evidenced that, at 300°C, a mixture of CoO şi Co_3O_4 is formed, a mixture that at 400 şi 700°C oxidizes into a single Co_3O_4 phase(JCPDS chart 42-1467 [24]).

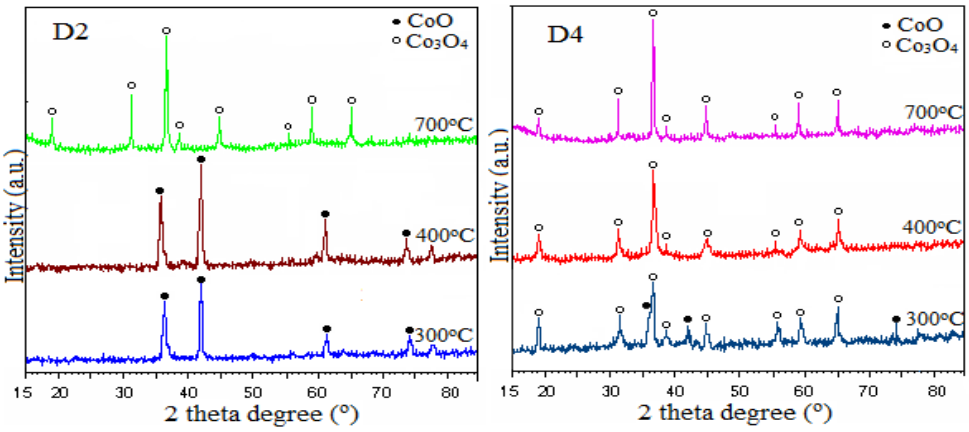

Figure 6. XRD spectra for samples D_2 and D_4 calcined at 300, 400 and 700°C for 3h

If the $Co(NO_3)_2$ - $C_2H_6O_2$ solutions are directly heated to a high temperature, a strongly exothermic redox reaction occurs, leading to the formation of a complex combination with an abundant release of nitrogen oxides. A thermal decomposition of this complex combination (auto combustion, reductive atmosphere) then follows. The obtained residue contains CoO as a single phase, regardless of the utilised precursor [22]. The median diameter of the crystallites were calculated from the XRD data for the samples calcined at 400 şi 700°C using the Scherrer equation [26].

The average crystallite size was calculated from the XRD data using Debye-Scherrer formula [26]:

$$D_{XRD} = \frac{C\,\lambda}{\beta_{1/2}\cos\theta} \qquad (1)$$

where D is the average crystallite size, $\beta_{1/2}$ is the broadening of full width at half maximum intensity (FWHM) of the main intense peak (311) in radian, C=0.9 for spherical particles θ is the Bragg angle, λ is the X-ray wavelength. At 400°C, the cobalt oxide crystallite diameter is 18,4 nm pentru D_2 si 19,1 nm pentru D_4, whereas at 700°C, it is 27,7 nm for sample D_2 and 28,1 nm for D_4. The cobalt oxide nanocrystallite diameter grows with a rise in temperature.

The SEM images for precursor D_4, thermally treated at 400 and 700°C (Figure 7), show an agglomeration of nanoparticles into micrometric aggregates.

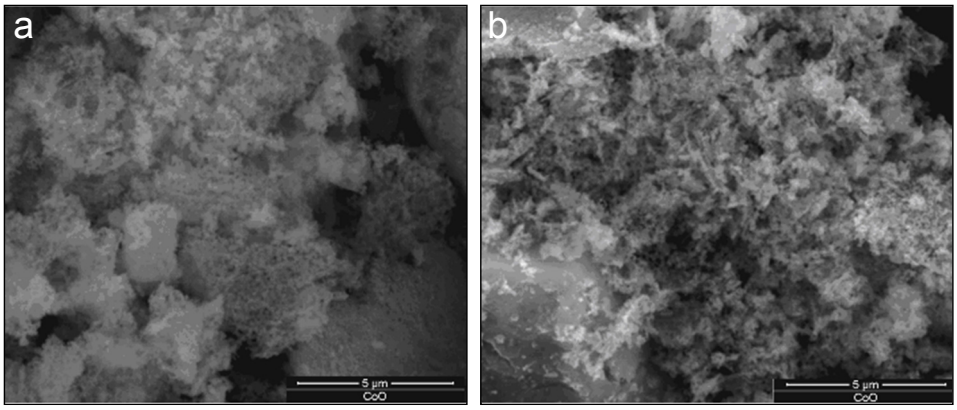

Figure 7. SEM images for precursor D_4 thermally treated at: (a) 400°C and (b) 700°C

CONCLUSIONS

This study highlights the formation of some carboxylate or hydro carboxylate complexes, through the redox reaction between $Co(NO_3)_2$ and diol. According to the utilized NO_3^- **:** ethyleneglycol molar ratio and the nature of the diol, single compounds or compound mixtures were obtained. The metal-organic precursor thermal decomposition method has the advantage of working at a low temperature, a temperature at which the precursors are thermally decomposed, leading to low crystallization oxide compounds. These compounds are highly reactive, being able to lead to the formation of crystalized CoO systems following further thermal treatments. FTIR analysis and the acido-basic studies have confirmed the formation of carboxylate and hydrocarboxylate compounds, single phased or in a combination. Electrometric titrations have also the advantage of automation, increasing the analysis throughput and securing the consistent quality of the results. Regardless of the nature of the precursor, the decomposition occurs up to 300^{o}C, generating a reductive atmosphere according to the nature of the precursor. During the thermal decomposition of the precursors, the reductive atmosphere leads to redox processes Co(II)→Co(0) →CoO or Co_3O_4, which stabilize into a single phase. The XRD diffraction spectra showed that CoO, Co_3O_4 are obtained in either a single phase or a combination, according to the thermal treatment and nature of the precursor. The CoO and Co_3O_4 crystallite median diameter calculation shows that, with the synthesis conditions and thermal treatment, cobalt oxide nanoparticles up to 30 nm in diameter are obtained.

EXPERIMENTAL SECTION

The reagents used in synthesis were: $Co(NO_3)_2 \cdot 6H_2O$ and ethylene glycol (EG=$C_2H_6O_2$) of purity p.a. (Merk). In the redox reaction between ethylene glycol and metallic nitrates, ethylene glycol ($C_2H_6O_2$) may be oxidized by NO_3^- ions to carboxylate anions (oxalate, glyoxylate, glycolate), according to the equations (1) ÷ (3), with the corresponding NO_3^- : $C_2H_6O_2$ molar ratios:

1) $3C_2H_4(OH)_2+8NO_3^-+2H^+ \rightarrow 3C_2O_4^{2-}+8NO+10H_2O$ ➔ EG : NO_3^- = 1: 2,67 oxalate anion
2) $C_2H_4(OH)_2+2NO_3^-+H^+ \rightarrow C_2H_3O_4^-+2NO+2H_2O$ ➔ EG : NO_3^- = 1: 2 glyoxylate anion
3) $3C_2H_4(OH)_2+4NO_3^-+H^+ \rightarrow 3C_2H_3O_3^-+4NO+5H_2O$ ➔ EG : NO_3^- = 1:1.33 glycolate anion

There were prepared 4 samples with different molar ratios (NO_3^- **:** EG), as presented in Table 2.

Table 2. Sample preparation correlated to the NO_3^-:EG molar ratio and 1-3 equations

Sample	Mol no. NO_3^-	Mol no. EG	Correlated to reaction 1	Correlated to reaction 2	Correlated to reaction 3
D_1	4	1	exces NO_3^-:1.33	Exces NO_3^-:2.0	exces NO_3^-:2.67
D_2	2	1	exces EG:0.25	stoechiometric	exces NO_3^-:0.67
D_3	1.33	1	exces EG:0.50	exces EG:0.34	stoechiometric
D_4	1	1	exces EG:0.62	exces EG:0.5	exces EG:0.25

The synthesis method consists in dissolving cobalt nitrate in the corresponding EG amount followed by controlled heating at temperatures higher than 100°C. At these temperatures, the redox reaction starts accompanied by nitrogen oxid emission (brown-reddish gas).

The redox reaction initiation temperature is around 140°C, the reaction being energetic, an important actor being the catalytic role of cobalt. According to the molar ratio (NO_3^- **:** EG), the reaction can be more or less controled, leading to a reaction product that is hard to isolate (it presents a high combustion tendency) . The reaction compounds were mantained at a 140°C temperature until the cessation in the release of brown gas (NO_x) (end of the reaction).

The obtained powders were milled and washed in acetone to remove any reactant excess. The obtained products were characterised through thermal analysis, FTIR spectrometry and acido-basic titrations (conductometric and pH-metric).

For the conductometric and potentiometric titrations, 0,2 mmols of Co(II) were used, with and addition of 10,0 cm^3 HCl 0.1M. The conductometric and potentiometric titrations were carried out with NaOH 0.1M.

The obtained nanocomposites were analyzed by thermogravimetry (TG), derivative thermogravimetry (DTG) and differential thermal analysis (DTA) using a SDT Q600 type instrument. The analysis was carried out in air, up to 1000°C at 10 °C min^{-1} using alumina standards.

The FTIR spectra were recorded on 1% KBr pellets using a Spectrum BX II spectrometer.

The XRD patterns were recorded using a high resolution Bruker D8 Advance diffractometer with Cu Kα1 ($\lambda_{CuK\alpha1}$=1,54056 Å) radiation.

The nanoparticle size was determined by transmission electron microscopy (TEM) using a Jeol JEM1010 with a resolution of 0.35 nm, equipped with a digital image recording system, a photographic film image recording system and a high resolution scanner.

The acido-basic properties of the precursors were studied through acido-basic titrations, conductometric and pH-metric, using a Crison MM41 multimeter.

REFERENCES

1. S.M. Ansari, R.D. Bhor, K.R. Pai, D. Sen, S. Mazumder, K. Ghosh, Y.D. Kolekar, *Applied Surface Science*, **2017**, 414, 171.
2. B.M. Mogudi, P. Ncube, R. Meijboom, *Applied Catalysis B: Environmental*, **2016**, 198, 74.
3. M.M. Durano, A.H. Tamboli, H. Kim, *Colloids and Surfaces A: Physicochemical and Engineering Aspects*, **2017**, 520, 355.
4. S. Harish, K. Silambarasan, G. Kalaiyarasan, A.V.N. Kumar, J. Joseph, *Material Letters*, **2016**, 165, 115.
5. J.M. Xu, J. Zhang, B.B. Wang, F. Liu, *Journal of Alloys and Compounds*, **2015**, 619, 361.
6. R.F. Klein Gunnewiek, C. Floriano Mendes, R.H. Goldschmidt Aliaga Kiminami, *Advanced Powder Technology*, **2016**, 27, 1056.
7. A. Ashok, A. Kumar, R.R. Bhosale, M.A.H. Saleh, U.K. Ghosh, M. Al-Marri, F.A. Almomani, M.M. Khader, *Ceramics International*, **2016**, 42, 12771.
8. S. Sun, X. Zhao, M. Yang, L. Ma, X. Shen, *Nanomaterials*, **2015**, 5, 2335-2347.
9. H.K. Lin.,H.C Chiu,H.C.Tsai,S.H.Chien,C.B. Wang, *Catalysis Letters* **2003**, 88, 3.
10. R.V. Narayan, V. Kanniah A. Dhathathreyan, *Journal of Chemical Sciences*, **2006**, 118:2, 179.
11. A.M. Garrido Pedrosa, M.J.B. Souza, D.M.A. Melo, A.S. Araujo, L.B. Zinner, J.D.G. Fernandes, A.E. Martinelli, *Solid State Sciences*, **2003**, 5, 725.
12. M. Pang, G. Long, S. Jiang, Y. Li, W. Han, B. Wang, X. Liu, Y. Xi, D. Wang, F. Xu, *Chemical Engineering Journal*, **2015**, 280, 377.
13. M. Montazerozohori, A. Masoudiasl, S. Farokhiyani, S. Joohari, P. McArdle, *Ultrasonic Sonochemistry*, **2017**, 38, 134.
14. F. Grillo, M.M. Natile, A. Glisenti, *Applied Catalysis B: Enviromental*, **2004**, 48, 267.
15. Y. Zhan, C. Yin, W. Wang, G. Wang, *Materials Letters*, **2003**, 57, 3402.
16. L. Zhang, D. Xue, C. Gao, *Journal of Magnetism and Magnetic Materials*, **2003**, 267, 111.
17. J. Jiu, Y. Ge, X. Li, L. Nie, *Materials Letters*, **2002**, 54, 260.
18. K. Vojisavljevic, S. Wicker, I. Can, A. Bencan, N. Barsan, B. Malic, *Advanced Powder Technology*, **2017**, 28, 1118.
19. H. Yang, Y. Hu, X. Zhang, G. Qiu, *Materials Letters*, **2004**, 58, 387.
20. Z.W. Yhao, Z.P. Guo, H.K.Liu, *Journal of Power Sources*, **2005**, 147, 264.
21. C.Y. Su, W.J. Lan, C.Y. Chu, X.J. Liu, W.Y. Kao, C.H. Chen, *Electrochimica Acta*, **2016**, 190, 588.
22. M. Stefanescu, T. Dippong, M. Stoia, O. Stefanescu, Journal of Thermal Analisys and Calorimetry, 2008, 94:2, 389.
23. K. Shalini, A.U. Mane, S.A. Shivashankar, M.Rajeswari, S.Choopun, Journal of Crystal Growth, 2001, 231, 242.
24. Joint Committee on Powder Diffraction Standards. International Center for Diffraction Data, 1999.
25. . E. Lima Jr., E.L. Winkler, D. Tobia, H.E. Troiani, R.D. Zysler, E. Agostinelli, D. Fiorani, *Chemistry of Materials,* **2012**, 24:3, 512.
26. L. Wang, M. Lu, Y. Liu, J. Li, M. Liu, H. Li, *Ceramic International*, **2015** 41, 4176.